

# A comparison of empirical and mechanistic models for wheat yield prediction at field level in Moroccan rainfed areas

Achraf Mamassi <sup>1,2</sup>, Marie Lang <sup>1</sup>, Bernard Tychon <sup>1</sup>, Mouanis Lahlou <sup>3</sup>,  
Joost Wellens <sup>1</sup>, Mohamed El Gharous <sup>2</sup>, H el ene Marrou <sup>\*,4</sup>

<sup>1</sup> Spheres Research Unit, University of Li ege, Arlon B-6700, Belgium;

<sup>2</sup> AgroBioSciences Program, Mohammed VI Polytechnic University, Benguerir 43150, Morocco;

<sup>3</sup> Department of Statistics and Computer Science, Institute of Agronomy and Veterinary Hassan II, Rabat 10101, Morocco;

<sup>4</sup> UMR AGAP Institut, Univ Montpellier, CIRAD, INRAE, Institut Agro, F-34398 Montpellier, France ;

\* Corresponding author's email [helene.marrou@supagro.fr](mailto:helene.marrou@supagro.fr)

  The Author(s) 2023. Published by Oxford University Press on behalf of the Annals of Botany Company.

This is an Open Access article distributed under the terms of the Creative Commons Attribution License (<https://creativecommons.org/licenses/by/4.0/>), which permits unrestricted reuse, distribution, and reproduction in any medium, provided the original work is properly cited.

## Abstract

In the context of climate change, in-season and longer-term yield predictions are needed to anticipate local and regional food crises and propose adaptations to farmers' practices. Mechanistic models and machine learning are two modelling options to consider in this perspective. In this study, regression (MR) and Random Forest (RF) models were calibrated for wheat yield prediction in Morocco, using data collected from 125 farmers' wheat fields. Additionally, MR and RF models were calibrated both with or without remotely-sensed leaf area index (LAI), while considering all farmers' fields, or specifically to agroecological zoning in Morocco. The same farmers' fields were simulated using a mechanistic model (APSIM-wheat). We compared the predictive performances of the empirical models and APSIM-wheat. Results showed that both MR and RF showed rather good predictive quality (NRMSEs below 35%), but were always outperformed by APSIM model. Both RF and MR selected remotely-sensed LAI at heading, climate variables (maximal temperatures at emergence and tillering), and fertilization practices (amount of nitrogen applied at heading) as major yield predictors. Integration of remotely-sensed LAI in the calibration process reduced NRMSE of 4.5% and 1.8 % on average for MR and RF models respectively. Calibration of region specific models did not significantly improve the predictive. These findings lead to the conclusion that mechanistic models are better at capturing the impacts of in-season climate variability and would be preferred to support short term tactical adjustments to farmers' practices, while machine learning models are easier to use in the perspective of mid-term regional prediction.

**Keywords:** yield prediction, empirical model, machine learning, APSIM-wheat, model comparison, Morocco.

## 1. Introduction

Ongoing climate change has reinforced the need to deliver crop yield predictions over short or longer time horizons (Crane-Droesch, 2018; Hasegawa et al., 2022). As extreme climatic events are more frequent and unpredictable (Savin et al., 2022), farmers need to take tactical decisions in-season to adapt their practices according to the expected production levels and production costs. Over several years, cropping practices may also require adaptation to cope with the local evolution of mean temperatures and rainfall distribution. In the rainfed areas of Morocco, farmers are particularly vulnerable to climate change. Recurrent droughts, aggravated by limited access to fertilizer, are responsible for highly variable crop yields and large yield gaps (Bregaglio et al., 2015; Henao and Baanan, 1999; Roy et al., 2003). Rainfed cereal production represents 80% of the total cereal production of the country (Shroyer et al., 1990), putting the food and economic balances of the country at risk.

Model-assisted decision-making in agriculture can reduce farmers' vulnerability to climatic risks and support adaptation to fluctuations in market inputs, the allocation of subsidies, and the recommendation of efficient and sustainable management practices for farmers (Asseng et al., 2019; De Wit et al., 2013; Kasampalis et al., 2018; Wang et al., 2014). National or regional crop yield prediction systems have been developed to support farmers and other stakeholders of the food chain, using numerical models. Two types of modeling approaches have been reported in the literature on yield prediction: i) Process-based approaches (i.e., mechanistic models) that represent the processes involved in crop development, growth, resource allocation, and the interactions between these through equations (Basso et al., 2013; Graeff et al., 2012; Jones et al., 2017). For example, the Global Yield Gap Atlas maps potential yield for major food crops in a large number of countries across the world, using processed based crop model simulations ([www.yieldgap.org](http://www.yieldgap.org)). ii) Empirical approaches that relate grain yield to agronomic and environmental factors (i.e., climate, soil, crop management information, etc.) including simple statistical relations (e.g., multiple regression analysis) (Palm, 1994; Thompson, 1969) or complex statistical algorithms (e.g., machine learning algorithms) (Droutsas et al., 2022; Marques Ramos et al., 2020; Son et al., 2022). For example, in Morocco, the national prediction system CGMS-MAROC, coordinated by the National Institute of Agriculture (INRA) produces maps of expected wheat production across Morocco, every year, using empirical models ([Downloaded from <https://academic.oup.com/insilicoplants/advance-article/doi/10.1093/insilicoplants/diad020/7390631> by guest on 12 November 2023](http://www.cgms-</a></p></div><div data-bbox=)

maroc.ma/). It is worthy to note that in this second category, the degree of empiricism varies between model based statistical approach in which predictors or distributions can be set based on biological assumptions to purely algorithmic.

Crop simulation models are valuable tools to predict yield in variable soil and climatic contexts and to support the adaptation of cropping practices. They can provide better understanding of the interactions between the major processes of the soil-plant-climate continuum and its global functioning at a daily time step. However, they often require a large number of input parameters (Cavalariis et al., 2021), which makes their deployment at large geographic scales over a variety on agroecosystems costly due to the logistics and financial resources needed to acquire parameter values (Makowski et al., 2006; Varella et al., 2010).

Conversely, empirical models estimate yield at a cropping season time step and can be easily used in research studies that target broad geographic ranges. The statistical approach provides a simple qualitative understanding of the links between grain yield measurements and environmental variables through regression and correlation analyses (Oteng-Darko et al., 2013), mainly represented in past studies by climate variables and remotely-sensed vegetation indices or biophysical variables (e.g., leaf area index - LAI, normalized difference vegetation index - NDVI, etc.) (Andarzian et al., 2008; Bolton and Friedl, 2013; Son et al., 2022).

High throughput data gathering methods employing remote sensing and satellite images have reshaped yield modeling over the past 10 years and diminished the divide between empirical and crop simulation models. The number of spectral indicators linked to crop state that may be integrated into empirical models has significantly increased as a result of recent technology advancements (Launay and Guerif, 2005; de Wit and van Diepen, 2007; Huang et al., 2019). Likewise, the integration of remotely obtained vegetation indexes into crop modeling pipelines has made it possible to reduce the degree of uncertainty in predictions of national yields (Luo et al., 2023).

Overall, empirical models are simpler to use, with a reduced number of parameters and possibly shorter calculation time requirements compared to crop models (Sultan et al., 2010). However, agronomic recommendations can be difficult to infer from these types of models that bypass the relations between climate, practices, and soil on one hand, and crop functioning on the other (Heil et al., 2018; Jones et al., 2001). This difficulty is increased by the possibility of identifying different sets of predictors for yield with equivalent performance using machine learning approaches. This is particularly the case with multivariate regression

models, and results from the collinearity among variables used in the model (Lischeid et al., 2022). Additionally, the vast majority of simple or complex statistical models used worldwide for yield prediction are non-spatial (Qu et al., 2022). They provide unique sets of selected environmental predictors of yield for an entire region; whilst – from an agronomic perspective – climatic, pedological, and management determinants of yield are known to vary across these large geographic regions. Simple customization of empirical models could outperform this limitation if zoning of the region of interest into sub-regions with homogenous climate conditions, soil status, or practices exists, so that different sets of predictors could be independently selected for each sub-region. In Morocco, zoning of the wheat production area was delimited by the FAO, within the framework of Strategy for the Conservation and Restoration of Agricultural Land (ISCRAL), which divides the Moroccan rainfed wheat production areas into four main climatic areas mainly defined by annual rainfall (i.e., favorable, unfavorable, intermediate, and mountain rainfed areas) (Akka, 2006; Harbouz et al., 2019; MAPMDREF, 2008).

The objective of the present study is to compare the predictive capacity of empirical models (multiple regression (MR) and random forests (RF) models) and a process-based model (APSIM-wheat model) for wheat yield across the rainfed areas of Morocco and discuss their suitability for different modeling objectives. The precision of the different prediction methods and sets of selected predictors will be compared, and the effect of recent advances in remote sensing technologies on the prediction gap between the empirical and process-based approaches will be assessed by integrating (1) the effect of incorporating a satellite-based vegetation index (LAI) in MR and RF models, (2) the effect of stratifying the dataset into different climatic sub-regions of Morocco for calibration of sub-region-specific empirical models. The performances of both improved and original empirical models as well as the mechanistic model will be discussed in the light of the time horizon targeted for prediction and support to farmers' decision-making.

## 2. Materials and Methods

### 2.1. Study area

### **Ble 3**

Morocco covers about 710,850 km<sup>2</sup>, and most of the country (93%) is characterized by an arid to semi-arid climate (Dahan et al., 2012). The agricultural production zones in Morocco are located between the mountains (Rif and Atlas), the Atlantic Ocean, and the Mediterranean

Sea. In the present study, 125 farmers' wheat fields were selected randomly across the main Moroccan rainfed areas based on the FAO's ISCRAL zoning (i.e., favorable (with precipitation >400 mm), intermediate (300–400 mm), and unfavorable rainfed areas (<300 mm) (Figure 1), and monitored during three cropping seasons (from 2018 to 2021). The selected farmers' fields represent a diversity of conditions (i.e., soil, management practices, and climatic conditions) (Figure 1) under the Moroccan rainfed areas, to ensure robust calibration and evaluation processes of both empirical and mechanistic models. The datasets were assembled from fieldwork conducted in the framework of the "SoilPhorLife" project and "Al Moutmir" program led by the Office Chérifien des Phosphates (OCP group).

## 2.2. Datasets

### 2.2.1 Phenological stages observations and grain yield measurement

During the three growing seasons, the main wheat phenological stages were monitored in the farmers' wheat fields based on Zadoks scale (Zadoks et al., 1974). To achieve an accurate scoring of each field as a whole, Zadoks scale scores were identified at 10 locations in each field, selected along a zigzag pattern.

Actual grain yield (Table 1) was measured at harvest in each farmer's field by harvesting five samples of 1 m<sup>2</sup> selected randomly across the field based on Bell and Fisher's methodology (Bell and Fischer, 1994).

### 2.2.2 Meteorological data

Daily maximum and minimum temperatures and daily rainfall were extracted from three sources. Weather station-based data were provided by the Office Régional de Mise en Valeur Agricole (ORMVA) and from a public website ([www.tutitempo.net](http://www.tutitempo.net)) (Tutitempo Network, S.L.) that offers data from airport weather stations. Since daily solar radiation was not available at most of these weather stations, data were completed with daily global radiation extracted from the satellite-based platform of NASA's Prediction of Worldwide Energy Resources (POWER) Project (<https://power.larc.nasa.gov/data-access-viewer/>) with a resolution of 0.5°×0.5° (i.e. about 50×50 km) (Sparks, 2018; Zhang et al., 2008). For each field, the closest weather station was chosen to represent the field's meteorological conditions. Using 15

different weather stations allowed to keep the distance between a field and the corresponding weather station below 50 km.

For each field, climatic variable variables were calculated by aggregating daily weather data over the main develop phase of wheat as recorded in the field (see section 2.2.1): (1) emergence (Z0 to Z20), (2) tillering (Z20 to Z30), (3) elongation (Z30 to Z50), (4) heading and anthesis, (Z50 to Z70), and (5) grain filling and maturity (Z70 to Z90). Cumulative rainfall (R1 to R5), means of maximum daily temperatures (Tmax1 to Tmax5), minimum daily temperatures (Tmin1 to Tmin5) and the cumulative growing degree days (GDD1 to GDD5) were calculated for each development phase and each field (Table 2). Moreover, the total cumulative precipitation (Rtot), the means of maximum (Tmax) and minimum (Tmin) daily temperature and the total cumulative growing degree days (GDDtot) were calculated for the entire crop cycle (i.e., from sowing date to harvesting date) (Table 2). The purpose of calculating these auxiliary variables was to capture yield potential as determined by wheat variety and local climate through GDD variables, as well as the effect of the main abiotic stresses (water stress, heat stress, and cold stress) for each development phase estimated through Tmin1 to Tmin5, Tmax1 to Tmax5, and R1 to R5 variables. Cumulative incident radiation available during each phenological stage was not considered due the uncertainty of this climatic variable (estimated from a satellite-based meteorological dataset) and the presence of a high collinearity effect between global radiation and maximum temperatures.

### 2.2.3 Soil data

Soil samples were collected in each field before the sowing date, at two depths (maximum depth depending on soil development, and in most cases less than 60 cm). Variables related to soil chemical properties (available-P (P), exchangeable-K (K), organic matter (OM), and pH) were determined standard procedures. Data were averaged over the two soil layers, using soil layer thickness as weights) for each field and each variable (Table 2).

### 2.2.4 Crop management data

The main crop management input variables, used during the calibration of empirical models and to parameterize the APSIM-wheat crop model, describe farmers' fertilization practices as recommended by experts. Crop management variables include the wheat cultivar and sowing date, amount of nitrogen-, phosphorus-, and potassium-based deep fertilizers applied at sowing date (respectively, N0, P<sub>2</sub>O<sub>5</sub>, and K<sub>2</sub>O), and the amount of nitrogen top-dressing fertilizer applied at tillering stage (N1) and at heading stage (N2). Total applied

nitrogen ( $N_{tot} = N_0 + N_1 + N_2$ ) and the total top-dressing nitrogen ( $N_d = N_1 + N_2$ ) were calculated and also used to calibrate empirical models.

### 2.2.5 Wheat growth satellite-based parameters

Sentinel-2 satellite images covering the monitored farmers' wheat fields during the three crop seasons (from 2018 to 2021) were downloaded from the Copernicus platform (<https://scihub.copernicus.eu/dhus/>) (European Space Agency). Sentinel-2 optical imagery provides a series of products with high temporal (5 days), spatial (10 to 60 m), and spectral (13 bands) resolution adapted for field-scale monitoring (Mohamed Sallah et al., 2019; Zhao et al., 2020).

Due to the large number of monitored fields, we extracted satellite images for two specific dates that represent determinant phenological stages, framing the period of maximum vegetative growth: at Z30 (end of tillering/start of elongation) and Z50 (end of elongation/start of heading). Only images with cloud cover lower or equal to 15% were considered. Due to the 5-day time resolution of Sentinel, the temporal uncertainties for variables extracted from satellite images were equal to 3 days. Unfavorable cloud cover (>15%) can occasionally increase this uncertainty, forcing us to skip overcast images and use images with low cloud cast on close dates. The downloaded images were preprocessed using the Sentinel Application Platform (SNAP) software (version 8.0.0) (<https://step.esa.int/main/toolboxes/snap/>) (European Space Agency), freely provided by Sentinel. Images underwent sequential pre-processing steps: resampling and creating subsets. Then, a SNAP algorithm was applied to compute and extract a leaf area index (LAI) raster map from each image. LAI was calculated based on spectral bands with a spatial resolution ranging between 10 to 20 meters. Finally, field polygons were delimited, excluding borders, and LAI was averaged over the pixel of each field polygon.

## 2.3. Calibration of empirical models

### 2.3.1. Modeling strategies for calibration of MR and RF models

Data collected in the field and derived from the soil and weather dataset for each field were compiled into a database (Table 1).

To test the possibility of integrating the spatial and temporal variation of the main determinants of wheat yield, two different modeling strategies were tested to split the dataset into a calibration and an evaluation subset:



- Extraction of one generic model covering the whole range of monitored farmers' fields across the rainfed wheat-growing area in Morocco (**S1**). The generic model was obtained by stratifying the available field data set: crop seasons (2019, 2020, and 2021) represent the strata, and 70% of the data from each of the three strata was used to calibrate models while 30% was used to evaluate the models.
- Extraction of three region-specific models for each of the rainfed agroclimatic areas (**S2**) (i.e., favorable, intermediate, and unfavorable). Region-specific (or agroclimate-specific) models were extracted using 70% of the observations while 30% of the dataset was used to evaluate those specific models.

To ensure the robustness of the comparisons between MR and RF models, both types of models were built on the same calibration and evaluation datasets described by the two strategies (S1 and S2). Modeling strategy (S1) was considered as the baseline for empirical models, compared to (S2) and models incorporating satellite-based LAI variables (Section 2.3.4).

### 2.3.2. Multiple regression models

Regression models with one predicted variable and more than one independent predictive variable are known as multivariate linear regression analysis (MR). The corresponding model is formulated as follows:

$$Y = b_0 + b_1.X_1 + \dots + b_i.X_i + \dots + b_n.X_n$$

where  $Y$  is the predicted variable,  $X_i$  represents  $n$  distinct independent variables (predictors), and  $b_i$  is the estimated regression coefficients.

Simple stepwise linear regression analyses were conducted using IBM-SPSS Statistics software (v 25.0) (SPSS Inc.) to examine whether independent quantitative variables (Table 1) were successful in predicting the dependent variable (wheat yield) and to assess the quality of contributions of each predictive variable. Assumptions of linearity, normal distribution, and multicollinearity of the predictor variables were verified. The model that minimized the minimum standard in the absence of multicollinearity was selected by the stepwise algorithm as the most appropriate to predict yield. The variance inflation factor "VIF" was calculated to interpret the multicollinearity, and VIF values under 2.5 were considered to represent an acceptable level of collinearity based on the literature (Fomby et

al., 1984). Finally, relative standardized estimators ( $\hat{\beta}_i$ ) were used to evaluate the contributions of individual predictors to the variation of yield. Relative standardized estimators of effects in the MR models were obtained by calculating the ratio between estimators for each predictor and the maximum of all estimators ( $\hat{b}_i$ ) in the selected model. Overall, the use of  $\beta$  values to estimate the predictors' relative importance is conditioned by the hypothesis of absence of multicollinearity (Cosnefroy and Sabatier, 2011), which was our second rule of MR model selection during the calibration process.

### 2.3.3. Random forests model

A set of random forests models was designed in R, version 4.1.2 (<https://cran.r-project.org/>), using the same variables as the MR model. Similarly, two modeling strategies were tested (see Section 2.3.3). The “caret” package, version 6.0-90 (Kuhn, 2022) was used throughout the procedure.

In a random forests model, a set of trees – in our case 500 – is built in a training phase and the outcome of the model is obtained by averaging the output of all the trees (Breiman, 2001). This operation was realized on the calibration samples described in section 2.3.1. The principle behind the random forests procedure is to increase the performance of the model by combining the outputs of a large number of different, average-performing models (Breiman, 1996). The variety in the models (trees) is obtained through two elements containing a random component. First, each tree is built on a randomly selected fraction (two-thirds) of the training dataset (calibration sample) by bootstrap aggregating (bagging) while the remaining part of the dataset (out-of-bag sample) is used to assess the prediction error of the tree (Breiman, 2001). Metrics describing the performance of the model in the training phase are reported here as “calibration results”. A second random effect is introduced at each node when the best split is determined among the variables. In the case of the random forests algorithm, only a randomly-selected sample of the independent variables is used at each node. In the models, the number of variables, controlled by the parameter “mtry”, was set as equal to the square root of the number of independent variables (Strobl et al., 2009), rounded to the nearest integer, in our case 6.

Random forests models feature the computation of a variable called permutation feature importance, a metric used to evaluate the impact of a variable on the model's performance. Permutation importance is based on the principle that if a variable is not important in the model, randomly permutating its values will not affect the model's performance, while it will

if the variable is important. The metric therefore represents the difference in model accuracy before and after permutation and grows larger as variables are more important (Breiman, 2001). In this study, the “cforest” method, from the R package party version 1.3-9 (Hothorn et al., 2006; Strobl et al., 2008, 2007) was used. This algorithm was designed to improve the estimation of importance in the presence of correlated predictors (Hothorn et al., 2006; Strobl et al., 2008, 2007). Finally, the performance of the final model (i.e., the average of the 500 trees) was assessed using the evaluation samples described in section 2.3.1 and by computing the metrics defined in section 2.5.

#### 2.3.4. Integration of satellite-based wheat LAI dataset into empirical models

To assess the impact of integrating the satellite-based wheat LAI on the statistical models' structure (choice and weight of the selected predictors) and performance for grain yield estimation, the calibration and evaluation of both MR and RF models was repeated including (with) or excluding (without) satellite-based LAI determinations at Z30 (LAI-Z30) and at Z50 (LAI-Z50) as input variables, in addition to variables related to climate, soil, and fertilizing practices. The comparison of the two approaches allowed us to quantify the degree of improvement in the models' potential for yield prediction through the incorporation of satellite-based information. Satellite-based LAI was preferred to NDVI or other remote sensing vegetation indices based on previous unpublished commercial exploration work conducted for an insurance company in Morocco. This choice was also supported by Abi Saab et al. (2019) who compared, under Mediterranean conditions, the correlation between winter wheat biomass as measured in the field and five remotely sensed vegetation indexes derived from Sentinel 2. They found that LAI was notably more correlated to biomass compared to NDVI.

#### 2.4. Mechanistic model: APSIM-wheat

APSIM “Agricultural Production Systems Simulator” (Keating et al., 2003) is a crop growth model that integrates, at a daily time step, the effect of soil, climate, crop cultivar, and crop management on interconnected processes (development, growth, resource allocation, and effect of abiotic stresses) involved in the elaboration of final yield (Ahmed et al., 2016; Keating et al., 2003). It has been employed to simulate a wide range of crops with a focus on addressing global challenges such as climate change and food and energy security, as it expresses the response of crops to meteorological, soil, and biological factors (He et al., 2017; Mohanty et al., 2012; Zhao et al., 2014). Moreover, it has been widely used in ex-ante

studies to explore the effect of crop management strategies such as fertilization, irrigation, weed management and control, land planning, or crop rotation. The detailed development history of APSIM was reported by Gaydon (2014).

Mamassi et al. (2012) previously conducted calibration and evaluation of the APISM-wheat model in the Moroccan context, using the same dataset as in the present study. The same parameterization procedure was applied in the present study: plant parameters and soil parameters were inferred from on-site measurement for each of the 125 farmers' fields that were simulated, and complemented by data from the literature, and open access data bases. Plant parameters were estimated separately for the five cultivars planted in the whole sample of farmer fields then calibrated according to a three step procedure: i) exploring influential and non-influential crop cultivars parameters to identify the parameters that required calibration, ii) using an Australian cultivar (also cultivated in Mediterranean conditions to set default values for unknown plant coefficients, iii) using the trial-and-errors simplified approach to adjust the plant parameters values. Calibration process was done by adjusting successively crop phenology, leaf area development and yield, as per Boote's systematic approach (Boote, 1999; Li et al., 2018) , and iv). Daily climate data (temperatures and precipitations) originated from the closest weather station of each field with a maximum distance of 50 km between the field and the weather station. Daily global radiation was extracted from NASA's Prediction Of Worldwide Energy Resources (NASA's POWER project) (<https://power.larc.nasa.gov/data-access-viewer/>). The detailed procedure used for APSIM-wheat model calibration and evaluation were reported in Mamassi et al. (2022).

## 2.5. Evaluation metrics

Statistical metrics were computed to evaluate the uncertainty of both empirical (RF and MR, generic or region-specific) and mechanistic (APSIM-wheat) models after calibration and validation phases: the root mean square error (RMSE) and the normalized root mean square error (NRMSE) as indicators of model precision, as well as the coefficient of determination ( $R^2$ ) as an indicator of accuracy as per Eq. 1, 2, and 3 respectively.

$$\text{RMSE} = \sqrt{\frac{1}{n} \sum_{i=1}^n [x_{s_i} - x_{m_i}]^2} \quad (1)$$

$$\text{NRMSE} = \frac{\sqrt{\frac{1}{n} \sum_{i=1}^n [x_{s_i} - x_{m_i}]^2}}{\bar{x}_m} \times 100 \quad (2)$$

$$R^2 = 1 - \frac{\sum_{i=1}^n [x_{s_i} - (\hat{a} \cdot x_{m_i} + \hat{b})]^2}{\sum_{i=1}^n [x_{m_i} - \bar{x}_m]^2} \quad (3)$$

where  $x_{m_i}$  is the measured values,  $x_{s_i}$  is the simulated values,  $\bar{x}_m$  is the mean of the observed value,  $n$  is the number of observations (i.e., fields), and  $\hat{a}$  and  $\hat{b}$  are the estimators of the simple linear regression between models simulated values and observed or measured values in real field.

RMSE and NRMSE were calculated in R (R Core Team, 2020), while  $R^2$  of MR models were obtained using IBM-SPSS Statistics software (v 25.0) (SPSS Inc.). For evaluating the benefit of incorporating satellite-based data as an input in MR and RF models, RMSE, NRMSE, and  $R^2$ , were computed for each case.

### 3. Results

#### 3.1. Comparison between empirical and mechanistic models

The indicators of predictive capacity of the calibrated and evaluated APSIM-wheat model for wheat yield in Moroccan rainfed areas are depicted in Figure 2; further details are available in Mamassi et al. (2022). The overall comparison between the empirical and mechanistic models showed that APSIM-wheat outperformed the baseline empirical models (**S1**, i.e. RF and MR generic models that were calibrated over the whole rainfed wheat-growing region without LAI variables), and the region specific models in favorable areas (**S2-Fav**). However, in the intermediate and unfavorable rainfed areas of Morocco, the best predictive performances were achieved by region-specific MR models when integrating the satellite-based variables (i.e., **S2-with-Int/Unfav**), with RMSEs equal to 0.47 and 0.17 t.ha<sup>-1</sup>, respectively.

### 3.2. Structure and predictive quality of generic empirical models (S1) without LAI variables (baseline models).

“Baseline models” (S1) refers to RF and MR generic models that were calibrated over the whole rainfed wheat-growing region in Morocco, and including only variables measured on the ground (without LAI variables) as possible predictors (Figures 2b and 3b). Quality metrics calculated on the calibration dataset showed good to acceptable predictive quality for both MR and RF baseline models. The lowest NRMSE value was obtained for the MR model (NRMSE = 24.9%). High  $R^2$  values generally exceeding 0.7 (Figure 2b) were obtained for both MR and RF models, indicating good model accuracy.

After the model calibration process, the validation of models using independent datasets aimed to verify their potential for predicting wheat yield in Moroccan rainfed areas (Figure 3). RF and MR baseline models showed almost identical wheat yield estimation performances with RMSEs ranging between 0.8 and 0.9 t.ha<sup>-1</sup> (Figure 3b) corresponding to NRMSE below 35%, while  $R^2$  exceeded 0.8 in both cases. The values of RMSE, NRMSE, and  $R^2$  obtained in the model evaluation step confirmed that both MR and RF calibrated baseline models had rather good predictive capacities for yield across the rainfed wheat production area in Morocco (Figure 2b).

Analysis of the models' structure (Figure 4b and supplemental material S2) indicates that the RF and MR calibration process selected the same predictors, and the best predictor variables for wheat yield, by decreasing order of importance, were: i) nitrogen fertilization, represented mainly by (Ntot) and (Nd) and ii) meteorological variables, mainly maximal temperature variables (Tmax1, Tmax2, and Tmax4) and cumulative rainfall variables (Rtot and R5).

Among the soil fertility and fertilization practice-related variables, only soil organic matter (OM) and soil pH (pH) were selected as predictors in models, with a secondary relative importance (Figure 4). Similarly, these variables were among those with the lowest relative and absolute importance in the RF baseline model (Supplemental Material – Table S1). Moreover, bivariate correlations between yield and predictive variables confirmed the weak contribution of K<sub>2</sub>O and to a lesser extent of P<sub>2</sub>O<sub>5</sub> to the explanation of yield variations (Supplemental material S3).

### 3.3. Effect of calibrating separate region-specific (or agroclimate-specific) models

Separately calibrating region-specific models for each agroclimatic zone (**S2**) did not significantly improve models' predictive power according to  $R^2$ , RMSE, and NRMSE values as calculated after calibration (Figure 2 and 3). Region-specific models, obtained with the MR algorithm with or without satellite-based variables had a better predictive quality than RF region-specific models, overall. Moreover, the RF algorithm failed to extract a model for the unfavorable rainfed areas (S2-Unfav). This was due to the limited number of fields in this region (9 fields only), which was inferior to the minimum number of observations needed by the algorithm to perform a split (parameter "minsplit" with a default value of 20). Although the algorithm allows setting one's own value for the parameter "minsplit", we decided not to alter the default value as designing an RF model based on such a limited sample would seriously limit its interpretability. As a result, the best fit proposed by the algorithm in this case was a constant value equal to the average yield (which prevented the computation of  $R^2$  and variable importance).

During the evaluation phase (Figure 2), nearly identical model predictive performances were obtained when applying the RF method for the two sampling strategies (S1 and S2), with NRMSE ranging between 26% and 34%, and  $R^2$  exceeding 0.8 (except for the S2-Unfav model that could not be calibrated with the RF approach). Conversely to what was observed after calibration, region-specific MR models outperformed the baseline models' (S1) precision in the case of favorable and intermediate rainfed areas (**S2-Fav/Int**), with NRMSE values ranging between 18% and 29% against NRMSE above 30% for (S1) models.  $R^2$  values remained above 0.7 for both MR and RF agroclimate-specific models (S2), except for the failure of the RF model in the unfavorable zone.

#### 4. Effect of integrating satellite-based data on model predictive quality

Calibration of generic and region-specific models with the MR and RF approaches was repeated when integrating LAI-Z30 and LAI-Z50 among the possible predictors of yield. Using remotely-sensed variables allowed us to minimize the NRMSE of models calculated on the evaluation dataset by 4.9% on average for MR models and 1.8% for RF models (Figure 2a). LAI-Z50 was selected as the most influential predictor variable for yield in most of RF and MR models (generic or region specific). On the contrary, LAI-Z30 parameter was not selected as a major predictor for any type of model (Figure 3a and supplemental material S3). The inclusion of LAI-Z50 in yield RF models mainly resulted in changing the order of

importance of predictors: maximum temperatures, total cumulated rainfall and N fertilization remained the main predictors together with LAI\_Z50. The inclusion of LAI-Z50 in MR model's was more disruptive of their structure, especially for region specific models: Incorporation of LAI-Z50 in MR models was compensated by the exclusion of soil fertility variables (OM, pH) and the reduction of the number of variables derived from maximum temperatures while cumulated rainfall in different phases appeared amongst the main predictors (Figure 3).

## 5. Discussion

### 4.1. Main environmental determinants of wheat yield in rainfed areas of Morocco.

The MR and RF models were fairly consistent in selecting climate, soil, and practice-related predictors for yield, even when creating models specific to different regions or agroclimates. Both generic models obtained using the S1 strategy and models specific to intermediate or unfavorable areas identified metrics derived from local rainfall and maximum temperatures as the primary determinant predictors of yield. This finding aligns with the understanding that water is the main limiting factor for cereal production in rainfed agricultural areas of Mediterranean countries, especially in regions where cumulative annual rainfall peaks at 400 mm (Perniola et al., 2015; Wani et al., 2009).

The significance of maximum temperature in predicting final yield can be interpreted through two pathways. Firstly, high temperatures can indicate the occurrence and severity of heat stress, which decreases yield. However, maximum temperature (Tmax) is also correlated with mean daily temperatures (Tmean) and daily incoming radiation, indicating its role in determining the duration of the crop cycle and the amount of radiation available to the crop. Due to these contrasting relationships between Tmax and final yield, its role as a primary predictor in RF and MR models is not immediately intuitive.

The MR and RF models also identified specific periods in the crop cycle when rainfall and maximum daily temperatures have a greater impact on final yield. Tmax2 (tillering phase) and Tmax4 (heading to flowering phase) were the temperature-related metrics most frequently selected as predictors in both types of models. These two metrics were consistently chosen in every RF model. Tmax1 (emergence to tillering) and Tmax3 (tillering to booting) were occasionally selected as secondary predictors in MR models. Thus, tillering and pre-flowering phases can be identified as the two phenological phases in wheat development that



are more likely to be subject to and sensitive to heat stress. The observation of maximum temperature dynamics throughout the crop cycle in rainfed areas in Morocco further supports these results, showing that maximum daily temperatures exceed 26°C on average from the start of February, which coincides with the full tillering phase and the beginning of elongation in wheat crops. Furthermore, several studies have demonstrated that heat stress during the vegetative growth phase of wheat reduces photosynthesis and dry matter accumulation, affecting the first yield components such as tiller and spike number per plant. Heat stress events during the pre-anthesis stages also increase pollen sterility, leading to a decrease in grain number (Farooq et al., 2011; Porter and Gawith, 1999).

In terms of rainfall, the RF model selected in-season total cumulative rainfall (R<sub>tot</sub>) as an important predictor of wheat yield, rather than stage-specific cumulative rainfall. This could be due to variations in soil water storage capacity across different fields, which can blur the relationship between the timing of rainfall and the effective timing of water stress, and its impact on yield. On the other hand, the MR models identified cumulative rainfall at specific stages, particularly R<sub>5</sub> (cumulative rainfall during the grain filling period), as a significant predictor variable for wheat yield. This discrepancy between the RF and MR models suggests an artificial correlation between R<sub>tot</sub> and R<sub>5</sub>, which could be responsible for the identification of R<sub>5</sub> as a predictor of final yield in MR models only. Dealing with multicollinearity using VIF results during MR model development is crucial to address this issue.

Nitrogen fertilization-related variables were considered the most important predictors in the baseline models (S1) for both MR and RF methods, indicating the prevalence of insufficient N fertilization of wheat in Morocco overall. In MR models without leaf area index (LAI) variables, total nitrogen (N<sub>tot</sub>) even emerged as the primary predictor of final yield. However, when LAI variables were included in MR and RF models, N-related variables

Soil fertility variables had limited importance as predictors of wheat yield in the MR and RF models. Only pH and organic matter (OM) were identified as secondary predictors in the MR models. The scarcity of soil variables in yield prediction studies may be due to the difficulty of obtaining relevant soil fertility data. However, better results have been achieved by combining crop management practices or soil data with meteorological and satellite-based crop growth data for field-scale yield estimation (Basso et al., 2013; Hunt et al., 2019). The significance of soil-related variables depends on the specific environment, such as temperate

or continental climates with minimal water stress or countries where fertilization practices mitigate nitrogen stress. For example, in Denmark, MR and RF models have been developed using soil properties like soil texture and organic carbon parameters to extract the national winter wheat yield map (Roell et al., 2020; Schjønning et al., 2018). Similarly, in the USA, a regression model identified soil organic matter and wilting point as significant contributors to corn yield variation (Ansarifar, 2021)

#### 4.2. Impact of integrating a satellite-based dataset on yield prediction accuracies

When considering LAI-related variables as predictors, LAI-Z50 consistently emerged as the primary predictor of yield in both RF and MR models. However, in this study, nitrogen fertilization and climate-related predictors persisted alongside LAI-Z50 in yield prediction models, despite addressing multicollinearity during calibration (Han et al., 2020; Li et al., 2022). This highlights the importance of integrating multiple variables as yield predictors in empirical models. LAI at end-tillering (LAI-Z30) did not emerge as a predictor, likely due to its strong correlation with LAI-Z50 and the variable growth dynamics compensating for low tillering LAI's impact on final yield. Notably, LAI-Z50 was not selected as a predictor only in region-specific RF models for favorable areas, potentially due to LAI-Z50 saturation resulting from high biomass density in late vegetative stages in these regions.

Although LAI-Z50 was consistently chosen as a major predictor, its integration only marginally improved the MR or RF models' predictive capacity, reducing NRMSE by 1.8 to 4.9%. The limited impact of integrating LAI-related variables could be attributed to the uncertainty surrounding these variables. The temporal resolution and image quality limitations of Sentinel-2 satellite data (5-day resolution and cloud cover) create incompatibilities with the actual observation dates of wheat development stages Z30 and Z50. Studies incorporating satellite-based variables such as NDVI, EVI, and LSWI have reported significant improvements in model accuracy (Balaghi et al., 2008; Han et al., 2020; Li et al., 2022; Marszalek et al., 2022; Meroni et al., 2021). These studies often cover large geographic regions and utilize low to medium quality images acquired at higher frequencies during key wheat vegetative stages or from sowing to harvesting. Enhancing the accuracy of RF and MR models in this study could be achieved by extracting satellite-based variables like LAI at higher frequencies, specifically during vegetative stages. Additionally, combining biophysical variables like LAI with satellite-based vegetation indices related to water and

nutrient status, such as NDWI, EVI, or LSWI, could further improve the models' accuracy in predicting yield at the field scale. These indices capture leaf moisture content and indicate the occurrence and severity of water stresses experienced by the crop (Gao, 1996; Marszalek et al., 2022; Xiao et al., 2006).

#### 4.3. Empirical vs. crop models: Different skills for different uses

##### 4.3.1. Predictive capacity

Past studies have reported higher model accuracy using empirical models instead of crop models to predict final yield (Estes et al., 2013; Prasad et al., 2022). However, in the present study, APSIM-wheat's predictive capacity was found to be higher than the tested empirical model (regardless of the method or calibration) in all pedoclimatic regions. NRMSE values with APSIM-wheat simulation were consistently below 20%. APSIM predictive quality was particularly better in unfavorable areas, while the RF approach struggled to fit a model and identify yield predictors in these regions, possibly due to a lower number of fields.

This underscores the need to improve the representation of water stress and its effects on crop processes, particularly in drought-prone areas. Future improvements in empirical models, including using high-frequency time series of satellite-based variables, higher-quality images, better representations of plant water stress, and region-specific calibrations could significantly increase their predictive performances. In particular, integrating high-resolution time series of state-related variables representing plant water status or topsoil water content may enhance RF, MR, or other machine learning models in such contexts (Proctor et al., 2022). The RF algorithm would be able to deal appropriately with this additional information as they can handle large datasets with numerous predictors. Besides, using a conditional approach (e.g. “cforest” function of the “party” package (Strobl et al., 2008)) ensures that variable importance is not biased toward correlated predictors. For MR models, increasing the number of predictors requires careful variable selection and handling of multicollinearity. Other machine learning methods like Gaussian process regression have shown higher performance in predicting yield (Bian et al., 2022), but it's uncertain if they can match the accuracy of a crop model like APSIM-wheat for Morocco's context.

##### 4.3.2. Capacity to support tactical adaptation of cropping practices in-season

MR or RF models use integrated variables that describe the entire crop cycle or specific moments within it. This property enables in-season yield prediction as soon as major

predictors are obtained for the ongoing cycle. The effectiveness of these models applicability in-season depends on the choice of best predictors. In this study, the baseline MR and RF models, which incorporate satellite-based variables, identified LAI-Z50 as the primary yield predictor, followed by Tmax2 and Ntot. These predictor values could be acquired in time to predict wheat yield a few days after the Z50 stage, occurring approximately two months before harvest in Morocco. RF agroclimate-specific models also allowed reasonably accurate yield prediction one to two months before harvest. However, the selection of Rtot and R5 as yield predictors in other models hindered their use for yield prediction before the grain filling stage. Overall, empirical models can appear more manageable for advising and supporting farmers compared to crop models. As a result, empirical models have been integrated into various tools and national operational systems for yield prediction in various countries (Fritz et al., 2019).

However, the machine learning approach cannot be considered a complete surrogate for a decision support tool as they struggle to determine the effects of practice changes. For example, beyond fertilization amounts, which are important predictors in RF and MR models in this study, farmers may modify the type of applied N-fertilizers or add other minerals to the crop. The RF and MR models cannot anticipate the effects of such decisions, requiring a recalibration of the models to understand the impact of tactical adaptations on yield. In contrast, crop models like APSIM-wheat are designed to represent the key processes that determine crop production, considering interactions with soil, climate, and farming practices (Asseng et al., 2013) which confers more robustness to models and the capacity to simulate a larger range of cropping practices. The primary challenge preventing crop models from being widely used as decision support tools lies in the extensive data requirements for field-specific parameterization, including access to local daily weather data from sowing to harvest that hinders the possibility of running the model during the cropping season. To address this challenge, an ensemble of possible (generated or historic) climatic series can be utilized to complete the climate file in season. This approach has been employed in the development of commercial decision support tools like the Yield Prophet (Hunt et al., 2006) (<https://www.yieldprophet.com.au/yp/Home.aspx>), which advises farmers in-season based on APSIM-wheat simulations. Another potential strategy involves integrating remote sensing data, such as satellite images, into crop modeling tools to improve model calibration and correct dynamical model outputs in season (Huang et al., 2019).

#### 4.3.3. Conservation of predictive capacity in the long term

In the long-term perspective, mechanistic crop models such as APSIM may be more efficient in predicting yield despite the introduction of improved cultivars in cropping systems. Crop model algorithms may be refined as new processes are integrated or revised into additional or improved modules but the core structure and principles of the model are not meant to be questioned by changes of the cropping environment or practices. Conversely, empirical models may require re-calibration and new predictors may be selected under changing environmental conditions, especially climate change, since climatic variables are major predictors for these models. Similarly, changes in fertilization practices, influenced by factors such as fertilizer and crop market prices or public policies, can impact the utility of some predictors, such as N<sub>2</sub> or N<sub>tot</sub> in the models assessed in this study. This, in turn, may increase model uncertainty if recalibration is not performed.

An open question arises regarding whether advancements in remote sensing technologies, automated data analysis pipelines, and computational capabilities will alleviate the need for frequent recalibration of empirical models. Such recalibration would otherwise be necessary every few years or across different regions, in order to accommodate contextual changes.

Several recent studies in the literature have suggested that, hybridization of process based models together with empirical models would result in improved predictive capacity both on long and short term (Maestrini et al., 2022; Shahhosseini et al. 2021; Zhang et al., 2023). While empirical models could support parameter estimation for crop models, crop output variable from crop models such as APSIM may be adequate predictors to statistical model and improve their predictive capacity.

## 6. Conclusion

While this work has not demonstrated a clear superiority of empirical models over a mechanistic model to predict crop yield in the case of wheat produced in the rainfed areas of Morocco, it evidenced the capacity of machine learning approaches to consistently identify the major yield determinants among a set of possible predictors, including when considering various algorithms. All the empirical models tested selected nitrogen fertilization and climatic variables as major yield predictors, before soil and crop management related variables: in

Morocco, rainfall and high temperatures are definitely the main determinants of yield, while soil and plant mineral status only explain marginal variation. Integrating recent advances in remote sensing, allowing the use of satellite-based vegetation indices such as LAI, into these models resulted in the incorporation of such variables as major predictors, before climatic predictors – but only slightly increased the models' predictive capacity. The attempt to make empirical models more site-specific to capture variation of yield determinants from one region to another was not conclusive. It is difficult to conclude if this is due to climatic determinants being actually the same all over the production area or due to a lack of sensitivity of empirical algorithms. However, this attempt revealed that resource-limited situations were equally difficult to model and predict for empirical and mechanistic models. Rather than clearly supporting the superiority of one type of model over another (empirical *vs.* mechanistic), the result of this work advocated a complementary use of one or another approach depending on data availability but also on the targeted time horizon for yield simulations (one-year *vs.* decades) and the modeling objectives (in-season guidance for tactical adaptation of crop management *vs.* ex-ante or ex-post assessment of practices).

Accepted Manuscript

## ACKNOWLEDGEMENTS

The authors thank the OCP Group and Prayon Group for funding this research project. The authors would like to express their appreciation to the engineers of the Al Moutmir Program-OCP for their logistical support, and to Moroccan local farmers for their assistance and indulgence.

## SOURCE OF FUNDING

This study was supported by financial funding from the sponsors of SoilPhorLife project (grant ID SoilPhorLife N°4): OCP Group, Prayon Group, University of Liège, and Mohammed VI Polytechnic University.

## CONFLICT OF INTEREST

The authors declare that they have no known competing financial interests or personal relationships that could influence the work reported in this paper.

## CONTRIBUTIONS BY THE AUTHORS

**Achraf Mamassi:** Conceptualization, methodology, data analysis, data curation, data visualization, writing - original draft, writing - review & editing. **Marie Lang:** Methodology, data analysis, data curation, writing - original draft, data visualization. **Hélène Marrou:** Conceptualization, methodology, writing - original draft, writing - review & editing, supervision. **Mouanis Lahlou:** Methodology, supervision. **Joost Wellens:** Methodology, supervision. **Mohamed El Gharous:** Funding acquisition. **Bernard Tychon:** Conceptualization, methodology, writing - review & editing, supervision, project administration, funding acquisition.

## DATA AVAILABILITY

The datasets generated and/or analyzed during the current study are available from the corresponding author on reasonable request. All data have been deposited on a github repository (link below) to which users may request access from the authors.

<https://github.com/Achraf-UM6P/Scripts-and-fields-dataset-ML-and-APSIM-for-yield-prediction/blob/fd67ef5444157a2a1abea699215bb6041778313c/Script%20and%20dataset.rar>

## LITERATURE CITED

- Abi Saab, M.T.; El Alam, R.; Jomaa, I.; Skaf, S.; Fahed, S.; Albrizio, R.; Todorovic, M. 2021. Coupling Remote Sensing Data and AquaCrop Model for Simulation of Winter Wheat Growth under Rainfed and Irrigated Conditions in a Mediterranean Environment. *Agronomy*. 11, 2265. <https://doi.org/10.3390/agronomy11112265>
- Ahmed, M., Akram, M.N., Asim, M., Aslam, M., Hassan, F. ul, Higgins, S., Stöckle, C.O., Hoogenboom, G., 2016. Calibration and validation of APSIM-Wheat and CERES-Wheat for spring wheat under rainfed conditions: Models evaluation and application. *Comput. Electron. Agric.* 123, 384–401. <https://doi.org/10.1016/j.compag.2016.03.015>
- Akka, A.E., 2006. Les politiques céréalières au Maroc . Meknes.
- Andarzian, B., Bakhshandeh, A.M., Bannayan, M., Emam, Y., Fathi, G., Alami Saeed, K., 2008. WheatPot: A simple model for spring wheat yield potential using monthly weather data. *Biosyst. Eng.* 99, 487–495. <https://doi.org/10.1016/j.biosystemseng.2007.12.008>
- Ansarifar, J., Wang, L., Archontoulis, S. V., 2021. An interaction regression model for crop yield prediction. *Sci. Reports* 2021 111 11, 1–14. <https://doi.org/10.1038/s41598-021-97221-7>
- Asseng, S., Ewert, F., Rosenzweig, C., Jones, J.W., Hatfield, J.L., Ruane, A.C., Boote, K.J., Thorburn, P.J., Rötter, R.P., Cammarano, D., Brisson, N., Basso, B., Martre, P., Aggarwal, P.K., Angulo, C., Bertuzzi, P., Biernath, C., Challinor, A.J., Doltra, J., Gayler, S., Goldberg, R., Grant, R., Heng, L., Hooker, J., Hunt, L.A., Ingwersen, J., Izaurralde, R.C., Kersebaum, K.C., Müller, C., Naresh Kumar, S., Nendel, C., O’Leary, G., Olesen, J.E., Osborne, T.M., Palosuo, T., Priesack, E., Ripoche, D., Semenov, M.A., Shcherbak, I., Steduto, P., Stöckle, C., Stratonovitch, P., Streck, T., Supit, I., Tao, F., Travasso, M., Waha, K., Wallach, D., White, J.W., Williams, J.R., Wolf, J., 2013. Uncertainty in simulating wheat yields under climate change. *Nat. Clim. Chang.* 3, 827–832. <https://doi.org/10.1038/nclimate1916>
- Asseng, S., Martre, P., Maiorano, A., Rötter, R.P., O’Leary, G.J., Fitzgerald, G.J., Girousse, C., Motzo, R., Giunta, F., Babar, M.A., Reynolds, M.P., Kheir, A.M.S., Thorburn, P.J., Waha, K., Ruane, A.C., Aggarwal, P.K., Ahmed, M., Balkovič, J., Basso, B., Biernath, C., Bindi, M., Cammarano, D., Challinor, A.J., De Sanctis, G., Dumont, B., Eyshi Rezaei, E., Fereres, E., Ferrise, R., Garcia-Vila, M., Gayler, S., Gao, Y., Horan, H., Hoogenboom, G., Izaurralde, R.C., Jabloun, M., Jones, C.D., Kassie, B.T., Kersebaum, K.C., Klein, C., Koehler, A.K., Liu, B., Minoli, S., Montesino San Martin, M., Müller, C., Naresh Kumar, S., Nendel, C., Olesen, J.E., Palosuo, T., Porter, J.R., Priesack, E., Ripoche, D., Semenov, M.A., Stöckle, C., Stratonovitch, P., Streck, T., Supit, I., Tao, F., Van der Velde, M., Wallach, D., Wang, E., Webber, H., Wolf, J., Xiao, L., Zhang, Z., Zhao, Z., Zhu, Y., Ewert, F., 2019. Climate change impact and adaptation for wheat protein. *Glob. Chang. Biol.* 25, 155–173. <https://doi.org/10.1111/gcb.14481>
- Balaghi, R., Tychon, B., Eerens, H., Jlibene, M., 2008. Empirical regression models using NDVI, rainfall and temperature data for the early prediction of wheat grain yields in Morocco. *Int. J. Appl. Earth Obs. Geoinf.* 10, 438–452. <https://doi.org/10.1016/j.jag.2006.12.001>
- Basso, B., Cammarano, D., Carfagna, E., 2013. Review of Crop Yield Forecasting Methods and Early Warning Systems, in: FAO (Ed.), *The First Meeting of the Scientific Advisory Committee of the Global Strategy to Improve Agricultural and Rural Statistics*. Rome, Italy, pp. 18–19.
- Bell, M.A., Fischer, R.A., 1994. Guide to plant and crop sampling: Measurements and observations for



- agronomic and physiological research in small grain cereals. CIMMYT, Mexico. <https://doi.org/http://hdl.handle.net/10883/1191>
- Bian, C., Shi, H., Wu, S., Zhang, K., Wei, M., Zhao, Y., Sun, Y., Zhuang, H., Zhang, X., Chen, S., 2022. Prediction of Field-Scale Wheat Yield Using Machine Learning Method and Multi-Spectral UAV Data. *Remote Sens.* 2022, Vol. 14, Page 1474 14, 1474. <https://doi.org/10.3390/RS14061474>
- Bolton, D.K., Friedl, M.A., 2013. Forecasting crop yield using remotely sensed vegetation indices and crop phenology metrics. *Agric. For. Meteorol.* 173, 74–84. <https://doi.org/10.1016/J.AGRFORMET.2013.01.007>
- Boote, K.J., 1999. Concepts for calibrating crop growth models, in: *DSSAT Version 3*. pp. 179–199.
- Bréda, N.J.J., 2008. Leaf Area Index. *Encycl. Ecol. Five-Volume Set* 2148–2154. <https://doi.org/10.1016/B978-008045405-4.00849-1>
- Bregaglio, S., Frasso, N., Pagani, V., Stella, T., Francone, C., Cappelli, G., Acutis, M., Balaghi, R., Ouabbou, H., Paleari, L., Confalonieri, R., 2015. New multi-model approach gives good estimations of wheat yield under semi-arid climate in Morocco. *Agron. Sustain. Dev.* 35, 157–167. <https://doi.org/10.1007/s13593-014-0225-6>
- Breiman, L., 2001. Random Forests. *Mach. Learn.* 2001 451 45, 5–32. <https://doi.org/10.1023/A:1010933404324>
- Breiman, L., 1996. Bagging predictors. *Mach. Learn.* 1996 242 24, 123–140. <https://doi.org/10.1007/BF00058655>
- Cavalaris, C., Megoudi, S., Maxouri, M., Anatolitis, K., Sifakis, M., Levizou, E., Kyparissis, A., 2021. Modeling of Durum Wheat Yield Based on Sentinel-2 Imagery. *Agron.* 2021, Vol. 11, Page 1486 11, 1486. <https://doi.org/10.3390/AGRONOMY11081486>
- Cosnefroy, O., Sabatier, C., 2011. Estimation de l'importance relative des prédicteurs dans un modèle de régression multiple. *Intérêt et limites des méthodes récentes. L'Année Psychol.* Vol. 111, 253–289. <https://doi.org/10.3917/ANPSY.112.0253>
- Crane-Droesch, A., 2018. Machine learning methods for crop yield prediction and climate change impact assessment in agriculture. *Environ. Res. Lett.* 13, 114003. <https://doi.org/10.1088/1748-9326/AAE159>
- Dahan, R., Boughlala, M., Mrabet, R., Laamari, A., Balaghi, R., Lajouad, L., 2012. A review of available knowledge on land degradation on Morocco. Rabat. <https://doi.org/http://doi.wiley.com/10.22004/ag.econ.253831>.
- De Wit, A., Hoek, S., Ballaghib, R., El Hairehc, T., Dong, Q., 2013. Building an operational system for crop monitoring and yield forecasting in Morocco. 2013 2nd Int. Conf. Agro-Geoinformatics Inf. Sustain. *Agric. Agro-Geoinformatics* 2013 466–469. <https://doi.org/10.1109/ARGO-GEOINFORMATICS.2013.6621964>
- de Wit, A.J.W., van Diepen, C.A., 2007. Crop model data assimilation with the Ensemble Kalman filter for improving regional crop yield forecasts. *Agric. For. Meteorol.* 146, 38–56. <https://doi.org/10.1016/j.agrformet.2007.05.004>
- Droutsas, I., Challinor, A.J., Deva, C.R., Wang, E., 2022. Integration of machine learning into process-based modelling to improve simulation of complex crop responses. *in silico Plants* 4, 1–16. <https://doi.org/10.1093/INSILICOPLANTS/DIAC017>

- Estes, L.D., Bradley, B.A., Beukes, H., Hole, D.G., Lau, M., Oppenheimer, M.G., Schulze, R., Tadross, M.A., Turner, W.R., 2013. Comparing mechanistic and empirical model projections of crop suitability and productivity: implications for ecological forecasting. *Glob. Ecol. Biogeogr.* 22, 1007–1018. <https://doi.org/10.1111/GEB.12034>
- European Space Agency, n.d. Sentinel-2 images [WWW Document]. URL <https://scihub.copernicus.eu/dhus/#/home> (accessed 7.19.22a).
- European Space Agency, n.d. STEP – Science Toolbox Exploitation Platform [WWW Document]. URL <http://step.esa.int/main/> (accessed 7.19.22b).
- Farooq, M., Bramley, H., Palta, J.A., Siddique, K.H.M., 2011. Heat Stress in Wheat during Reproductive and Grain-Filling Phases. *CRC. Crit. Rev. Plant Sci.* 30, 1–17. <https://doi.org/10.1080/07352689.2011.615687>
- Fomby, T.B., Johnson, S.R., Hill, R.C., 1984. Multicollinearity. *Adv. Econom. Methods* 283–306. [https://doi.org/10.1007/978-1-4419-8746-4\\_13](https://doi.org/10.1007/978-1-4419-8746-4_13)
- Fritz, S., See, L., Bayas, J.C.L., Waldner, F., Jacques, D., Becker-Reshef, I., Whitcraft, A., Baruth, B., Bonifacio, R., Crutchfield, J., Rembold, F., Rojas, O., Schucknecht, A., Van der Velde, M., Verdin, J., Wu, B., Yan, N., You, L., Gilliams, S., Mùcher, S., Tetrault, R., Moorthy, I., McCallum, I., 2019. A comparison of global agricultural monitoring systems and current gaps. *Agric. Syst.* 168, 258–272. <https://doi.org/10.1016/J.AGSY.2018.05.010>
- Gao, B.C., 1996. NDWI—A normalized difference water index for remote sensing of vegetation liquid water from space. *Remote Sens. Environ.* 58, 257–266. [https://doi.org/10.1016/S0034-4257\(96\)00067-3](https://doi.org/10.1016/S0034-4257(96)00067-3)
- Gaydon, D., 2014. The APSIM Model – An Overview, in: SAARC Agriculture Centre (Ed.), *The SAARC-Australia Project-Developing Capacity in Cropping Systems Modelling for South Asia*. Dhaka, Bangladesh, pp. 15–31.
- Gommes, R., El Hairech, T., Rossillon, D., Balaghi, R., 2009. Impact of climate change on agricultural yields in Morocco, in: (FAO) (Ed.), *World Bank - Morocco Study on the Impact of Climate Change on the Agricultural Sector*. Rome, pp. 1–105.
- Graeff, S., Link, J., Binder, J., Claupei, W., 2012. Crop Models as Decision Support Systems in Crop Production, in: *Crop Production Technologies*. InTech. <https://doi.org/10.5772/28976>
- Han, J., Zhang, Z., Cao, J., Luo, Y., Zhang, L., Li, Z., Zhang, J., 2020. Prediction of Winter Wheat Yield Based on Multi-Source Data and Machine Learning in China. *Remote Sens.* 2020, Vol. 12, Page 236 12, 236. <https://doi.org/10.3390/RS12020236>
- Harbouz, R., Pellissier, J.-P., Rolland, J.-P., Khechimi, W., 2019. *Rapport de synthèse sur l’agriculture au Maroc*. Rabat.
- Hasegawa, T., Wakatsuki, H., Ju, H., Vyas, S., Nelson, G.C., Farrell, A., Deryng, D., Meza, F., Makowski, D., 2022. A global dataset for the projected impacts of climate change on four major crops. *Sci. Data* 2022 91 9, 1–11. <https://doi.org/10.1038/s41597-022-01150-7>
- He, D., Wang, E., Wang, J., Robertson, M.J., 2017. Data requirement for effective calibration of process-based crop models. *Agric. For. Meteorol.* 234–235, 136–148. <https://doi.org/10.1016/j.agrformet.2016.12.015>
- Heil, K., Heinemann, P., Schmidhalter, U., 2018. Modeling the effects of soil variability, topography, and management on the yield of barley. *Front. Environ. Sci.* 6, 146. <https://doi.org/10.3389/FENV.2018.00146/BIBTEX>

- Henao, J., Baanan, C., 1999. Estimating Rates of Nutrient Depletion in Soils of Agricultural Lands of Africa. International Fertilizer Development Center, Muscle Shoals, Alabama, USA.
- Hothorn, T., Bühlmann, P., Dudoit, S., Molinaro, A., Van Der Laan, M.J., 2006. Survival ensembles. *Biostatistics* 7, 355–373. <https://doi.org/10.1093/BIOSTATISTICS/KXJ011>
- Huang, J., Gómez-Dans, J.L., Huang, H., Ma, H., Wu, Q., Lewis, P.E., Liang, S., Chen, Z., Xue, J.H., Wu, Y., Zhao, F., Wang, J., Xie, X., 2019. Assimilation of remote sensing into crop growth models: Current status and perspectives. *Agric. For. Meteorol.* 276–277, 107609. <https://doi.org/10.1016/J.AGRFORMET.2019.06.008>
- Huete, A., Didan, K., Miura, T., Rodriguez, E.P., Gao, X., Ferreira, L.G., 2002. Overview of the radiometric and biophysical performance of the MODIS vegetation indices. *Remote Sens. Environ.* 83, 195–213. [https://doi.org/10.1016/S0034-4257\(02\)00096-2](https://doi.org/10.1016/S0034-4257(02)00096-2)
- Hunt, J., van Rees, H., Hochman, Z., Carberry, P.S., Holzworth, D., Dalgliesh, N., Brennan, L.E., Poulton, P.L., van Rees, S., Huth, N.I., Peake, A., 2006. Yield Prophet® : an online crop simulation service, in: Turner, N., Acuna, T. (Eds.), *Proceedings of the Australian Agronomy Conference*. CSIRO, Perth.
- Hunt, M.L., Blackburn, G.A., Carrasco, L., Redhead, J.W., Rowland, C.S., 2019. High resolution wheat yield mapping using Sentinel-2. *Remote Sens. Environ.* 233, 111410. <https://doi.org/10.1016/J.RSE.2019.111410>
- Jones, J.W., Antle, J.M., Basso, B., Boote, K.J., Conant, R.T., Foster, I., Godfray, H.C.J., Herrero, M., Howitt, R.E., Janssen, S., Keating, B.A., Munoz-Carpena, R., Porter, C.H., Rosenzweig, C., Wheeler, T.R., 2017. Toward a new generation of agricultural system data, models, and knowledge products: State of agricultural systems science. *Agric. Syst.* 155, 269–288. <https://doi.org/10.1016/j.agry.2016.09.021>
- Jones, J.W., Keating, B.A., Porter, C.H., 2001. Approaches to modular model development. *Agric. Syst.* 70, 421–443. [https://doi.org/10.1016/S0308-521X\(01\)00054-3](https://doi.org/10.1016/S0308-521X(01)00054-3)
- Kasampalis, D., Alexandridis, T., Deva, C., Challinor, A., Moshou, D., Zalidis, G., 2018. Contribution of Remote Sensing on Crop Models: A Review. *J. Imaging* 4, 52. <https://doi.org/10.3390/jimaging4040052>
- Keating, B., Carberry, P., Hammer, G., Probert, M., Robertson, M., Holzworth, D., Huth, N., Hargreaves, J.N., Meinke, H., Hochman, Z., McLean, G., Verburg, K., Snow, V., Dimes, J., Silburn, M., Wang, E., Brown, S., Bristow, K., Asseng, S., Chapman, S., McCown, R., Freebairn, D., Smith, C., 2003. An overview of APSIM, a model designed for farming systems simulation. *Eur. J. Agron.* 18, 267–288. [https://doi.org/10.1016/S1161-0301\(02\)00108-9](https://doi.org/10.1016/S1161-0301(02)00108-9)
- Kuhn, M., 2022. *Caret: Classification and Regression Training*.
- Launay, M., Guerif, M., 2005. Assimilating remote sensing data into a crop model to improve predictive performance for spatial applications. *Agric. Ecosyst. Environ.* 111, 321–339. <https://doi.org/10.1016/j.agee.2005.06.005>
- Li, Z., Ding, L., Xu, D., 2022. Exploring the potential role of environmental and multi-source satellite data in crop yield prediction across Northeast China. *Sci. Total Environ.* 815, 152880. <https://doi.org/10.1016/J.SCITOTENV.2021.152880>
- Li, Z., He, J., Xu, X., Jin, X., Huang, W., Clark, B., Yang, G., Li, Z., 2018. Estimating genetic parameters of DSSAT-CERES model with the GLUE method for winter wheat (*Triticum aestivum* L.) production. *Comput. Electron. Agric.* 154, 213–221. <https://doi.org/10.1016/j.compag.2018.09.009>

- Lischeid, G., Webber, H., Sommer, M., Nendel, C., Ewert, F., 2022. Machine learning in crop yield modelling: A powerful tool, but no surrogate for science. *Agric. For. Meteorol.* 312, 108698. <https://doi.org/10.1016/J.AGRFORMET.2021.108698>
- Luo L., Sun S., Xue J., Gao Z., Zhao J., Yin Y., Gao F., Luan X., 2023. Crop yield estimation based on assimilation of crop models and remote sensing data: A systematic evaluation, *Agric. Systems.* 210, 103711, ISSN 0308-521X, <https://doi.org/10.1016/j.agry.2023.103711>.
- Maestrini, B., Mimić, G., van Oort, P.A.J., Jindo, K., Brdar, S., van Evert, F.K., Athanasiados, I., 2022. Mixing process-based and data-driven approaches in yield prediction. *Eur. J. Agron.* 139, 126569. <https://doi.org/10.1016/J.EJA.2022.126569>
- Makowski, D., Naud, C., Jeuffroy, M.H., Barbottin, A., Monod, H., 2006. Global sensitivity analysis for calculating the contribution of genetic parameters to the variance of crop model prediction. *Reliab. Eng. Syst. Saf.* 91, 1142–1147. <https://doi.org/10.1016/j.ress.2005.11.015>
- Mamassi, A., Marrou, H., El Gharous, M., Wellens, J., Jabbour, F.-E., Zeroual, Y., Hamma, A., Tychon, B., 2022. Relevance of soil fertility spatial databases for parameterizing APSIM-wheat crop model in Moroccan rainfed areas. *Agron. Sustain. Dev.* 2022 425 42, 1–16. <https://doi.org/10.1007/S13593-022-00813-4>
- MAPMDREF, 2008. Atlas de l'agriculture marocaine . Rabat. <https://www.agriculture.gov.ma/>
- Marques Ramos, A.P., Prado Osco, L., Elis Garcia Furuya, D., Nunes Gonçalves, W., Cordeiro Santana, D., Pereira Ribeiro Teodoro, L., Antonio da Silva Junior, C., Fernando Capristo-Silva, G., Li, J., Henrique Rojo Baio, F., Marcato Junior, J., Eduardo Teodoro, P., Pistori, H., 2020. A random forest ranking approach to predict yield in maize with uav-based vegetation spectral indices. *Comput. Electron. Agric.* 178, 105791. <https://doi.org/10.1016/J.COMPAG.2020.105791>
- Marszalek, M., Körner, M., Schmidhalter, U., 2022. Prediction of multi-year winter wheat yields at the field level with satellite and climatological data. *Comput. Electron. Agric.* 194, 106777. <https://doi.org/10.1016/J.COMPAG.2022.106777>
- Meroni, M., Waldner, F., Seguini, L., Kerdiles, H., Rembold, F., 2021. Yield forecasting with machine learning and small data: What gains for grains? *Agric. For. Meteorol.* 308–309, 108555. <https://doi.org/10.1016/J.AGRFORMET.2021.108555>
- Mohamed Sallah, A.H., Tychon, B., Piccard, I., Gobin, A., Van Hoolst, R., Djaby, B., Wellens, J., 2019. Batch-processing of AquaCrop plug-in for rainfed maize using satellite derived Fractional Vegetation Cover data. *Agric. Water Manag.* 217, 346–355. <https://doi.org/10.1016/j.agwat.2019.03.016>
- Mohanty, M., Probert, M.E., Reddy, K.S., Dalal, R.C., Mishra, A.K., Subba Rao, A., Singh, M., Menzies, N.W., 2012. Simulating soybean-wheat cropping system: APSIM model parameterization and validation. *Agric. Ecosyst. Environ.* 152, 68–78. <https://doi.org/10.1016/j.agee.2012.02.013>
- Oteng-Darko, P., Yeboah, S., Addy, S.N.T., Amponsah, S., Danquah, E., 2013. Crop modeling: A tool for agricultural research – A review. *J. Agric. Res. Dev.* 2, 1–6.
- Palm, R., 1994. Modèles agrométéorologiques : régression et analyse de la tendance, in: Séminaire Sur Les Méthodes de Prévion de Rendements Agricoles. Office for Official Publications of the European Communities, Villefranche-sur-Mer, France, pp. 67–76.
- Perniola, M., Lovelli, S., Arcieri, M., Amato, M., 2015. Sustainability in cereal crop production in

- mediterranean environments. *Sustain. Agro-Food Nat. Resour. Syst. Mediterr. Basin* 15–27. [https://doi.org/10.1007/978-3-319-16357-4\\_2/FIGURES/4](https://doi.org/10.1007/978-3-319-16357-4_2/FIGURES/4)
- Porter, J.R., Gawith, M., 1999. Temperatures and the growth and development of wheat: a review. *Eur. J. Agron.* 10, 23–36. [https://doi.org/10.1016/S1161-0301\(98\)00047-1](https://doi.org/10.1016/S1161-0301(98)00047-1)
- Prasad, N.R., Patel, N.R., Danodia, A., Manjunath, K.R., 2022. Comparative performance of semi-empirical based remote sensing and crop simulation model for cotton yield prediction. *Model. Earth Syst. Environ.* 8, 1733–1747. <https://doi.org/10.1007/S40808-021-01180-X/FIGURES/12>
- Proctor, J., Rigden, A., Chan, D., Huybers, P., 2022. More accurate specification of water supply shows its importance for global crop production. *Nat. Food* 2022 39 3, 753–763. <https://doi.org/10.1038/s43016-022-00592-x>
- Qu, M., Guang, X., Li, J., Liu, H., Zhao, Y., Huang, B., 2022. An Integrated Yield-Based Methodology for Improving Soil Nutrient Management at a Regional Scale. *Agron.* 2022, Vol. 12, Page 298 12, 298. <https://doi.org/10.3390/AGRONOMY12020298>
- R Core Team, 2020. A Language and Environment for Statistical Computing.
- Roell, Y.E., Beucher, A., Møller, P.G., Greve, M.B., Greve, M.H., 2020. Comparing a Random Forest Based Prediction of Winter Wheat Yield to Historical Yield Potential. *Agron.* 2020, Vol. 10, Page 395 10, 395. <https://doi.org/10.3390/AGRONOMY10030395>
- Roy, R.N., Misra, R.V., Lesschen, J.P., Smaling, E.M., 2003. Assessment of soil nutrient balance: Approaches and methodologies. Rome.
- Savin, R., Cossani, C.M., Dahan, R., Ayad, J.Y., Albrizio, R., Todorovic, M., Karrou, M., Slafer, G.A., 2022. Intensifying cereal management in dryland Mediterranean agriculture: Rainfed wheat and barley responses to nitrogen fertilisation. *Eur. J. Agron.* 137, 126518. <https://doi.org/10.1016/J.EJA.2022.126518>
- Schjønnning, P., Jensen, J.L., Bruun, S., Jensen, L.S., Christensen, B.T., Munkholm, L.J., Oelofse, M., Baby, S., Knudsen, L., 2018. The Role of Soil Organic Matter for Maintaining Crop Yields: Evidence for a Renewed Conceptual Basis. *Adv. Agron.* 150, 35–79. <https://doi.org/10.1016/BS.AGRON.2018.03.001>
- Shahhosseini, M., Hu, G., Huber, I., Archontoulis, S. V., 2021. Coupling machine learning and crop modeling improves crop yield prediction in the US Corn Belt. *Sci. Reports* 2021 111 11, 1–15. <https://doi.org/10.1038/s41598-020-80820-1>
- Shroyer, J.P., Ryan, J., Monem, M.A., El-Mourid, M., 1990. Production of fall-planted cereals in Morocco and technology for its improvement. *J. Agron. Educ.* 19, 32–40.
- Son, N.T., Chen, C.F., Cheng, Y.S., Toscano, P., Chen, C.R., Chen, S.L., Tseng, K.H., Syu, C.H., Guo, H.Y., Zhang, Y.T., 2022. Field-scale rice yield prediction from Sentinel-2 monthly image composites using machine learning algorithms. *Ecol. Inform.* 69, 101618. <https://doi.org/10.1016/J.ECOINF.2022.101618>
- Sparks, A., 2018. nasapower: A NASA POWER Global Meteorology, Surface Solar Energy and Climatology Data Client for R. *J. Open Source Softw.* 3, 1035. <https://doi.org/10.21105/joss.01035>
- Strobl, C., Boulesteix, A.L., Kneib, T., Augustin, T., Zeileis, A., 2008. Conditional variable importance for random forests. *BMC Bioinformatics* 9, 1–11. <https://doi.org/10.1186/1471-2105-9-307/FIGURES/4>
- Strobl, C., Boulesteix, A.L., Zeileis, A., Hothorn, T., 2007. Bias in random forest variable importance measures: Illustrations, sources and a solution. *BMC Bioinformatics* 8, 1–21. <https://doi.org/10.1186/1471-2105-8-25/FIGURES/11>

- Strobl, C., Malley, J., Tutz, G., 2009. An Introduction to Recursive Partitioning: Rationale, Application and Characteristics of Classification and Regression Trees, Bagging and Random Forests. *Psychol. Methods* 14, 323. <https://doi.org/10.1037/A0016973>
- Sultan, B., Bella-Medjo, M., Berg, A., Quirion, P., Janicot, S., 2010. Multi-scales and multi-sites analyses of the role of rainfall in cotton yields in West Africa. *Int. J. Climatol.* 30, 58–71. <https://doi.org/10.1002/JOC.1872>
- Thompson, L.M., 1969. Weather and Technology in the Production of Corn in the U. S. Corn Belt1. *Agron. J.* 61, 453–456. <https://doi.org/10.2134/AGRONJ1969.00021962006100030037X>
- Tutiempo Network, S.L., n.d. Climate Dataset.
- Varela, H., Guérif, M., Buis, S., 2010. Global sensitivity analysis measures the quality of parameter estimation: The case of soil parameters and a crop model. *Environ. Model. Softw.* 25, 310–319. <https://doi.org/10.1016/j.envsoft.2009.09.012>
- Wala, A.A., Jauad, E. kharraz, Gül, Ö., 2019. Morocco Water Report.
- Wang, E., Bell, M., Luo, Z., Moody, P., Probert, M.E., 2014. Modelling crop response to phosphorus inputs and phosphorus use efficiency in a crop rotation. *F. Crop. Res.* 155, 120–132. <https://doi.org/10.1016/j.fcr.2013.09.015>
- Wani, S.P., Rockstrom, J., Oweis, T., 2009. Rainfed agriculture: unlocking the potential. Wallingford, UK: CABI; Patancheru, Andhra Pradesh, India: International Crops Research Institute for the Semi-Arid Tropics (ICRISAT); Colombo, Sri Lanka: International Water Management Institute (IWMI).
- Xiao, X., Boles, S., Frohling, S., Li, C., Babu, J.Y., Salas, W., Moore, B., 2006. Mapping paddy rice agriculture in South and Southeast Asia using multi-temporal MODIS images. *Remote Sens. Environ.* 100, 95–113. <https://doi.org/10.1016/J.RSE.2005.10.004>
- Zadoks, J.C., Chang, T.T., Konzak, C.F., 1974. A decimal code for the growth stages of cereals. *Weed Res.* 14, 415–421. <https://doi.org/10.1111/j.1365-3180.1974.tb01084.x>
- Zhang, T., Chandler, W.S., Hoell, J.M., Westberg, D., Whitlock, C.H., Stackhouse, P.W., 2008. A Global Perspective on Renewable Energy Resources: Nasa's Prediction of Worldwide Energy Resources (Power) Project, in: *Proceedings of ISES World Congress 2007 (Vol. I – Vol. V)*. Springer Berlin Heidelberg, Berlin, Heidelberg, pp. 2636–2640. [https://doi.org/10.1007/978-3-540-75997-3\\_532](https://doi.org/10.1007/978-3-540-75997-3_532)
- Zhang, N., Zhou, X., Kang, M., Hu, B.-G., Heuvelink, E., Marcelis, L.F.M., Buckley, T., 2023. Machine learning versus crop growth models: an ally, not a rival. *AoB Plants* 15, 1–7. <https://doi.org/10.1093/AOBPLA/PLAC061>
- Zhao, G., Bryan, B.A., Song, X., 2014. Sensitivity and uncertainty analysis of the APSIM-wheat model: Interactions between cultivar, environmental, and management parameters. *Ecol. Modell.* 279, 1–11. <https://doi.org/10.1016/j.ecolmodel.2014.02.003>
- Zhao, Y., Potgieter, A.B., Zhang, M., Wu, B., Hammer, G.L., 2020. Predicting Wheat Yield at the Field Scale by Combining High-Resolution Sentinel-2 Satellite Imagery and Crop Modelling. *Remote Sens.* 12, 1024. <https://doi.org/10.3390/rs12061024>

**Figure 1. Location of the 125 monitored farmers' fields across agroecological zones in Morocco. (A) Distribution of cumulative annual rainfall across Morocco (Wala et al., 2019), (B) field locations and limits of the four agroclimatic zones in northern Morocco (favorable, intermediate, unfavorable, and mountain rainfed areas) (Gommes et al., 2009). RA: Rainfed Area.**

**Figure 2. Comparison of MR, RF, and APSIM-wheat models' predictive performances calculated on the evaluation independent dataset. Coefficient of determination ( $R^2$ ), root mean square error (RMSE), and normalized root mean square error (NRMSE) are the statistical indices used to evaluate and compare models' precision and accuracy, a) with and b) without integrating satellite-based variables. S1 refers to generic models while S2-Fav: favorable, S2-Int: Intermediate, and S2-Unfav: Unfavorable rainfed areas, refer to agroclimate-specific models, respectively for favorable, intermediate, and unfavorable agroclimatic areas.**

**Figure 3. Coefficient of determination ( $R^2$ ), root mean square error (RMSE) and normalized root mean square error (NRMSE) of multiple regression (MR) and random forests (RF) models calculated on the calibration dataset. S1: generic model. S2: region specific models with fav: favorable (>4000 mm per year), Int: intermediate (300 to 400 mm) and Unfav: unfavorable (<300 mm) rainfed areas. a) with and b) without integrating satellite-based variables during the calibration process.**

**Figure 4. Relative importance of the main predictors of wheat yield in multiple regression (MR) and random forests (RF) models when calibrated as: S1: generic models and S2: region-specific models with fav: for favorable, Int: for intermediate and Unfav: for unfavorable rainfed areas. a) with and b) without integrating satellite-based variables.**

**Table 1. Descriptive statistics for wheat yield in Moroccan rainfed areas. Figures in brackets indicate the number of fields in each zone.**

**Table 2. Variables used to calibrate the empirical models of yield prediction in Moroccan rainfed areas. R1 to R5: Cumulative rainfall, Tmax1 to Tmax5 : means of maximum daily temperatures, Tmin1 to Tmin5: means of minimum daily temperatures and GDD1 to GDD5: cumulative growing degree days, respectively at (1) emergence (Z0 to Z20), (2) tillering (Z20 to Z30), (3) elongation (Z30 to Z50), (4) heading and anthesis, (Z50 to Z70), and (5) grain filling and maturity (Z70 to Z90). Z0, Z30, Z50, Z70, Z90: developmental stages on Zadock's scale.**

Accepted Manuscript



**Table 1. Descriptive statistics for wheat yield in Moroccan rainfed areas. Figures in brackets indicate the number of fields in each zone.**

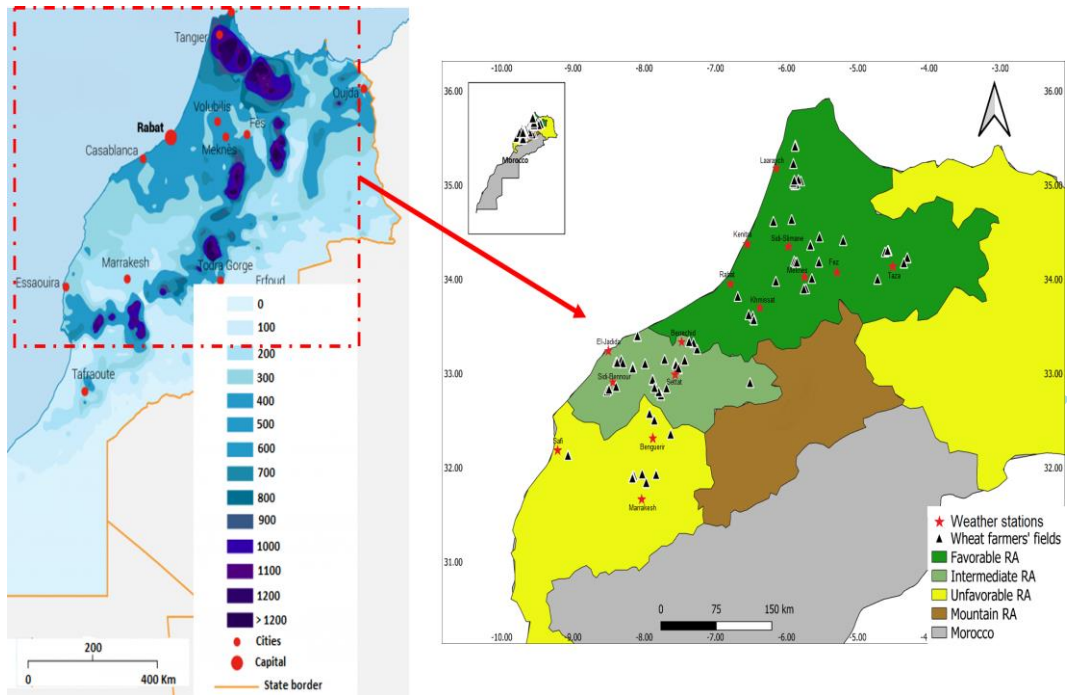
	Wheat yield (Mg.ha <sup>-1</sup> )			Overall
	Favorable rainfed areas (61)	Intermediate rainfed areas (44)	Unfavorable rainfed areas (20)	
<b>Mean</b>	3.74	1.81	0.67	2.57
<b>Median</b>	3.80	1.85	0.60	2.20
<b>Maximum</b>	7.10	3.80	1.40	7.10
<b>Minimum</b>	0.50	0.20	0.20	0.20
<b>SD</b>	1.70	1.04	0.40	1.82

Accepted Manuscript

**Table 2. Variables used to calibrate the empirical models of yield prediction in Moroccan rainfed areas. R1 to R5: Cumulative rainfall , Tmax1 to Tmax5 : means of maximum daily temperatures, Tmin1 to Tmin5: means of minimum daily temperatures and GDD1 to GDD5: cumulative growing degree days, respectively at (1) emergence (Z0 to Z20), (2) tillering (Z20 to Z30), (3) elongation (Z30 to Z50), (4) heading and anthesis, (Z50 to Z70), and (5) grain filling and maturity (Z70 to Z90). Z0, Z30, Z50, Z70, Z90: developmental stages on Zadock's scale.**

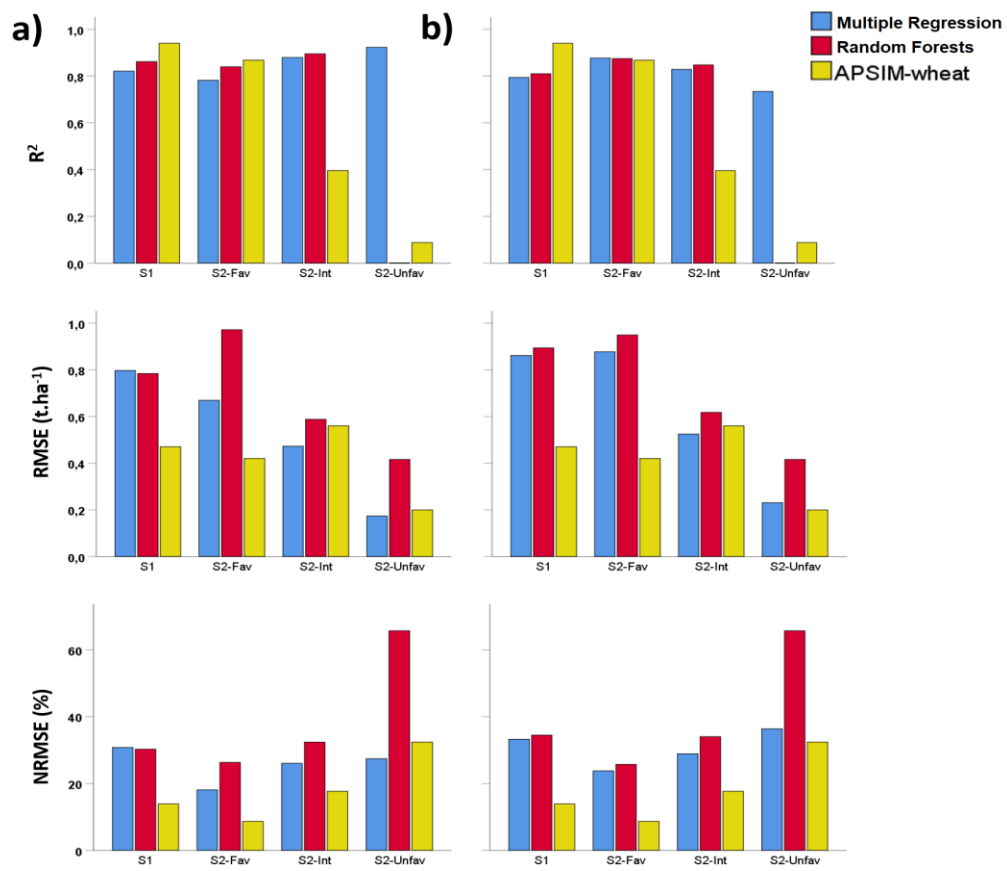
Data type	Variable	Symbol	Unit	Description
<b>Climate</b>	Cumulative rainfall	R1 to R5, Rtot	mm	See Section 2.2.1
	Minimum temperature	Tmax1 to Tmax5, Tmax	°C	
	Maximum temperature	Tmin1 to Tmin5, Tmin	°C	
<b>Soil fertility</b>	Organic matter	OM	%	See Section 2.2.2
	Available phosphorus	P	ppm	
	Exchangeable potassium	K	ppm	
	pH	pH	-	
<b>Crop management practices</b>	Cultivar	VAR	-	See Section 2.2.3
	Sowing dates	SD	Julian days	
	Nitrogen fertilization	N0, N1, N2, Nd, Ntot	kg.ha <sup>-1</sup>	
	Phosphorus fertilization	P <sub>2</sub> O <sub>5</sub>	kg.ha <sup>-1</sup>	
	Potassium fertilization	K <sub>2</sub> O	kg.ha <sup>-1</sup>	
<b>Duration of phenological stages</b>	Growing degree days	GDD1 to GDD5, GDDtot	C°.day <sup>-1</sup>	See Sections 2.2.1 and 2.2.4
	<b>Satellite-based metrics related to wheat growth</b>	Leaf area index	LAIZ30, LAIZ50	m <sup>2</sup> .m <sup>-2</sup> See Section 2.2.5

Figure 1



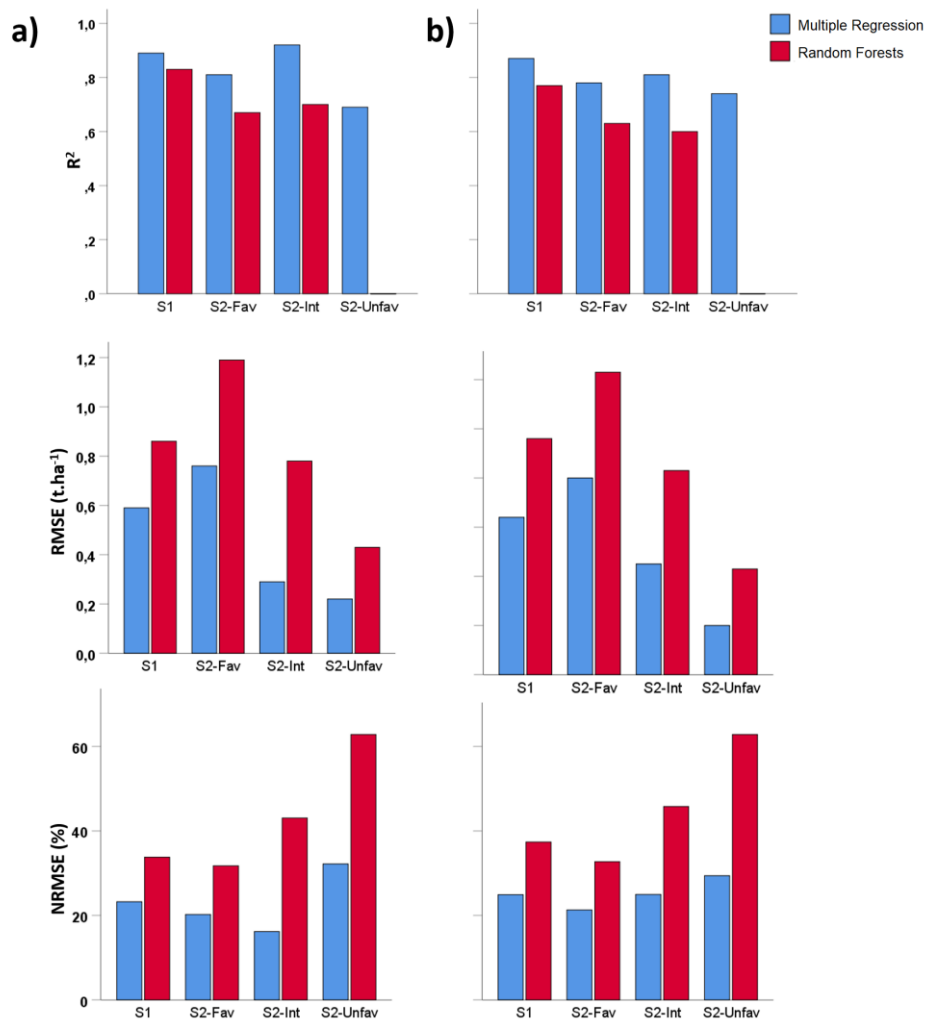
Accepted Manuscript

Figure 2



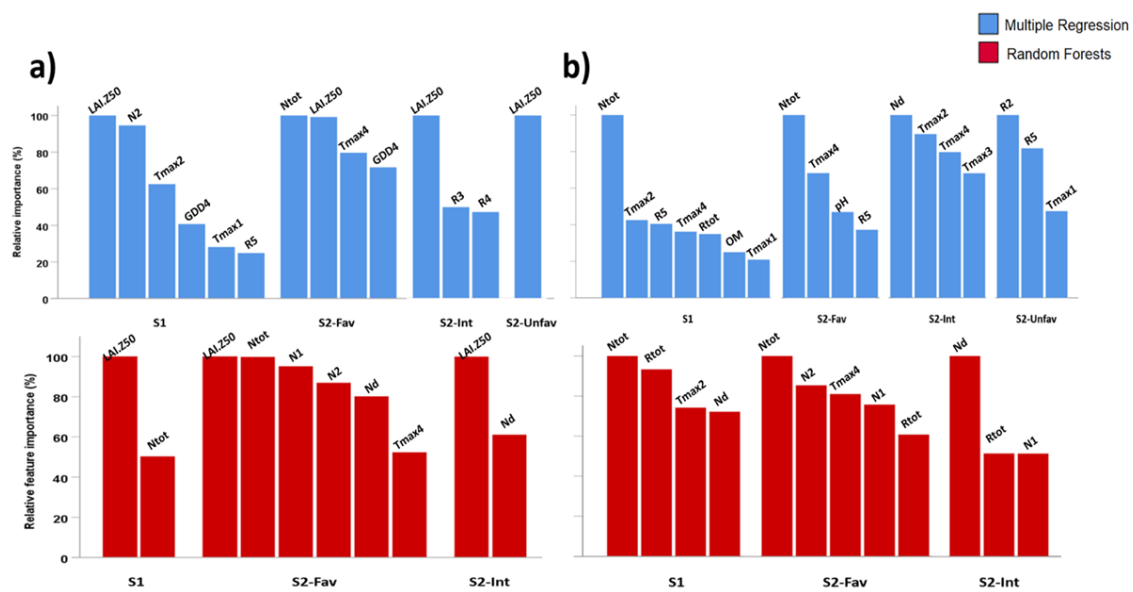
Accepted

Figure 3



Accept

Figure 4



Accepted Manuscript